NASA Technical Memorandum 87207

Nonlinear Bending-Torsional Vibration and Stability of Rotating, Pretwisted, Preconed Blades Including Coriolis Effects

K.B. Subrahmanyam, K.R.V. Kaza,
G.V. Brown, and C. Lawrence
Lewis Research Center
Cleveland, Ohio

January 1986

NASA

NONLINEAR BENDING-TORSIONAL VIBRATION AND STABILITY OF ROTATING, PRETWISTED, PRECONED BLADES INCLUDING CORIOLIS EFFECTS

K.B. Subrahmanyam,* K.R.V. Kaza, G.V. Brown and C. Lawrence
National Aeronautics and Space Administration
Lewis Research Center
Cleveland, Ohio 44135

E-2811

SUMMARY

The coupled bending-bending-torsional equations of dynamic motion of rotating, linearly pretwisted blades are derived including large precone, second degree geometric nonlinearities and Coriolis effects. The equations are solved by the Galerkin method and a linear perturbation technique. Accuracy of the present method is verified by comparisons of predicted frequencies and steady state deflections with those from MSC/NASTRAN and from experiments. Parametric results are generated to establish where inclusion of only the second degree geometric nonlinearities is adequate. The nonlinear terms causing torsional divergence in thin blades are identified. The effects of Coriolis terms and several other structurally nonlinear terms are studied, and their relative importance is examined.

INTRODUCTION

It is now widely recognized that the inclusion of geometric nonlinearities in the equations of motion of rotating elastic blades is necessary for a fair prediction of their dynamic characteristics. For the analysis of helicopter rotor blades, an appropriate set of nonlinear equations based upon Euler-Bernoulli theory was found to yield satisfactory results since the blades were essentially slender (refs. 1 to 5). However, there remain certain questions concerning the degree to which the geometric nonlinearities should be retained, and concerning the initial assumptions in prescribing an ordering scheme (refs. 6 to 7). Another area, somewhat similar dynamically, but further complicated due to the geometry, is the advanced turboprop blade dynamics (refs. 8 to 9). In contrast to helicopter rotor blades, the turboprop blades are more plate or shell-like, possess variable sweep along the span, and have smaller thickness ratios. Furthermore, the ratio of the rotational speed to the first nonrotating normal mode frequency of the turboprop blade is usually less than one, while the corresponding ratio for the helicopter blade can be somewhat more than one. Because of the unusual geometric features of the advanced turboprop blades, finite element methods are normally used. However, when finite element modeling is used, it is difficult to obtain a physical understanding of the complicating effects.

In order to determine the individual and combined effects of pretwist, sweep and rotation on the blades, parameteric studies are conducted by using a

---

*On leave from NBKR Institute of Science Technology, Mechanical Engineering Department, Vidyanagar 524413, India and presently Senior Research Associate, University of Toledo, Toledo, Ohio 43606.

simpler beam model in which the effects of sweep are incorporated by preconing the blade with respect to the plane of rotation. Precone, a component of sweep, is of the order of 50° for an advanced turboprop blade at the tip. Assuming constant precone, linear pretwist and steady rotational speed, the coupled nonlinear equations for bending-bending-torsional motion are derived by using the theory presented in references 3 and 4. In deriving the equations, it is assumed that the elongations and shears are negligible compared to unity and the squares of the derivative of the extensional deformation of the elastic axis is negligible compared to the square of the bending slopes. Shear deflection and rotary inertia effects are not considered. Geometric nonlinearities are retained up to second degree. Parametric results from the present beam theory for the special case of torsionally rigid blades (refs. 10 and 11) indicated excellent agreement with finite element model results generated by MSC/NASTRAN.

In the present paper, the important effect of torsional flexibility is addressed. A brief derivation of the coupled nonlinear equations of bending-bending-torsional motion are first presented. Next, implementation of the Galerkin method with nonrotating normal modes for the solution of the nonlinear steady state equations and the linearized perturbation equations is presented. Parametric results generated from the present beam theory are compared with similar results produced by MSC/NASTRAN. The limitations of restricting the geometric nonlinearities to second degree, and the effects of Coriolis forces for blades with various thickness ratios are shown. Results obtained from experimental tests are also presented for typical precone angles, rotational speed and setting angles. Finally, the accuracy of the present equations, the limits where the second degree geometric nonlinearities are adequate, and the parameters affecting the onset of instability are discussed.

EQUATIONS OF MOTION AND METHOD OF SOLUTION

Figure 1 shows a linearly pretwisted, preconed, and rotating blade of uniform rectangular cross section. The coupled bending-bending-torsional equations of motion for such a blade are derived by using the theory presented in reference 3, and by including large precone and linear pretwist over the blade length. When shear and rotary inertia effects are ignored, and second degree geometric nonlinearities and Coriolis effects are retained, such equations reduce to the following form (a list of notation is given in appendix B):

Flatwise bending:

$$m\ddot{w} + 2m\Omega \sin \beta_{pc}\dot{v} - (Tw')' - m\Omega^2 \sin^2 \beta_{pc} w$$

$$+ m\Omega^2 \left(k_{m2}^2 - k_{m1}^2\right) \cos 2\beta_{pc} \; (v' \sin \theta \cos \theta)'$$

$$+ m\Omega^2 \cos 2\beta_{pc} \left[w'\left(k_{m2}^2 \sin^2 \theta + k_{m1}^2 \cos^2 \theta\right)\right]'$$

$$+ m\Omega^2 \left(k_{m2}^2 - k_{m1}^2\right) \sin \beta_{pc} \cos \beta_{pc} \; (\phi \sin 2\theta)'$$

$$+ 2\Omega \cos \beta_{pc} \left[\dot{\phi}\left(mk_{m2}^2 \sin^2 \theta + mk_{m1}^2 \cos^2 \theta\right)\right]'$$

$$+ \left\{w'' \left[EI_{\eta\eta} \cos^2 \theta + EI_{\xi\xi} \sin^2 \theta + \phi \left(EI_{\xi\xi} - EI_{\eta\eta}\right) \sin 2\theta\right]\right.$$

$$\left. + v'' \left[\left(EI_{\xi\xi} - EI_{\eta\eta}\right)\left(\sin \theta \cos \theta + \phi \cos 2\theta\right)\right] - \phi' v' \; GJ\right\}''$$

$$= - m\Omega^2 \sin \beta_{pc} \cos \beta_{ps} \left(x - u_F\right) - \Omega^2 \sin \beta_{pc} \cos \beta_{pc} \left(mk_{m2}^2 \sin^2 \theta + mk_{m1}^2 \cos^2\theta\right)' \tag{1}$$

Edgewise bending:

$$m\ddot{v} - 2m\Omega \sin \beta_{pc}\dot{w} - m\Omega^2 v + \left(\phi' w'' GJ\right)' - 2m\Omega \cos \beta_{pc} \; \dot{u}_F \; - (Tv')'$$

$$+ 2\Omega \cos \beta_{pc} \left[\dot{\phi}(mk_{m2}^2 - mk_{m1}^2) \sin \theta \cos \theta\right]'$$

$$+ m\Omega^2 \left(k_{m2}^2 - k_{m1}^2\right) \cos 2\beta_{pc} \; (w' \sin \theta \cos \theta)'$$

$$+ m\Omega^2\left(k_{m2}^2 - k_{m1}^2\right) \sin \beta_{pc} \cos \beta_{pc}\left(\phi \cos 2\theta\right)'$$

$$- m\Omega^2 \sin^2\beta_{pc} \left[v' \left(k_{m2}^2 \cos^2 \theta + k_{m1}^2 \sin^2 \theta\right)\right]'$$

$$+ \left\{w''\left[\left(EI_{\xi\xi} - EI_{\eta\eta}\right)\left(\sin \theta \cos \theta + \phi \cos 2\theta\right)\right]\right.$$

$$\left. + v''\left[EI_{\eta\eta}\left(\sin^2 \theta + \phi \sin 2\theta\right) + EI_{\xi\xi} \left(\cos^2 \theta - \phi \sin 2\theta\right)\right]\right\}''$$

$$= -\Omega^2\left[\sin \beta_{pc} \cos \beta_{pc}\left(mk_{m2}^2 - mk_{m1}^2\right) \sin \theta \cos \theta\right]' \tag{2}$$

Torsion:

$$
\begin{aligned}
& mk_m^2\ddot{\phi} + m\Omega^2 \phi \cos^2 \beta_{pc}\left(k_{m2}^2 - k_{m1}^2\right) \cos 2\theta \\
&\quad + 2m\Omega \cos \beta_{pc} \left\{\left(k_{m2}^2 - k_{m1}^2\right) \dot{v}' \sin \theta \cos \theta \right. \\
&\quad \left. + \dot{w}'\left(k_{m2}^2 \sin^2 \theta + k_{m1}^2 \cos^2 \theta\right)\right\} + \left(EC_1 \phi''\right)'' - \left[EAk_A^2 u' \left(\theta'_{pt} + \phi'\right)\right. \\
&\quad \left. + EB_1 \theta_{pt}'^2 \phi' + GJ\phi' - v'w'' GJ\right]' + \left(mk_\lambda^4 \Omega^2 \cos^2 \beta_{pc} \phi'\right)' \\
&\quad + \left(EI_{\xi\xi} - EI_{\eta\eta}\right)\left[v''w'' \cos 2\theta + \left(w''^2 - v''^2\right) \sin \theta \cos \theta\right] \\
&\quad - m\Omega^2 \sin \beta_{pc} \cos \beta_{pc}\left(k_{m2}^2 - k_{m1}^2\right) v' \cos 2\theta \\
&\quad - m\Omega^2 \sin \beta_{pc} \cos \beta_{pc}\left(k_{m2}^2 - k_{m1}^2\right) w' \sin 2\theta \\
&\quad = - m\Omega^2 \cos^2 \beta_{pc}\left(k_{m2}^2 - k_{m1}^2\right) \sin \theta \cos \theta
\end{aligned}
\tag{3}
$$

Where:

$$
\begin{aligned}
T = - \int_x^L \Big[& m\, \Omega^2 w \sin \beta_{pc} \cos \beta_{pc} - 2\Omega \dot{v} \cos \beta_{pc} \\
& - \Omega^2 (R + x - u_F) \cos^2 \beta_{pc} - \ddot{u}_F \Big]\, dx
\end{aligned}
\tag{4}
$$

$$
u_F = \frac{1}{2}\int_0^x (v'^2 + w'^2)\, dx \tag{5}
$$

$$
EAu' = T - EA\left[k_A^2\, \phi'\theta'_{pt}\right] \tag{6}
$$

and

$$
\left.
\begin{aligned}
& m = \iint \rho\, dydz,\ A = \iint dydz,\ I_{\xi\xi} = \iint y^2 dydz,\ I_{\eta\eta} = \iint z^2 dydz, \\
& Ak_A^2 = \iint \left(y^2 + z^2\right) dydz,\ B_1 = \iint \left(y^2 + z^2\right)^2 dydz,\ C_1 = \iint \lambda^2 dydz, \\
& J = \iint \left\{\left(y - \lambda_z\right)^2 + \left(z + \lambda_y\right)^2\right\} dydz,\ mk_{m1}^2 = \iint \rho z^2 dydz, \\
& mk_{m2}^2 = \iint \rho y^2 dydz,\ k_m^2 = k_{m1}^2 + k_{m2}^2,\ ()' = \frac{\partial}{\partial x}(),\ \lambda_y = \frac{\partial \lambda}{\partial y},\ \lambda_z = \frac{\partial \lambda}{\partial z},\ \dot{()} = \frac{\partial}{\partial t}().
\end{aligned}
\right\}
\tag{7}
$$

In deriving the equations given above, an ordering scheme given in reference 3 is followed. Geometric nonlinear terms up through second degree only are retained. In general, terms up to $O(\epsilon^4)$ in the elastic forces and $O(\epsilon^2)$ in the inertial forces are needed in the bending equations. For the sake of verification, certain linear terms of the order $O(\epsilon^3)$ in the inertial forces are included in equations (1) and (2). However, these additional terms have been found to have an insignificant affect on the solutions and can be discarded safely. Considering the torsion equation, terms of the order $O(\epsilon^5)$ in the elastic forces and terms of the order $O(\epsilon^3)$ in the inertial forces forces together with the structural and inertial warping terms, [viz. $(EC_1\phi'')''$ and $(mk_A^4\Omega^2 \cos^2\beta_{pc}\, \phi')'$], are retained. A large number of higher order terms other than those shown in the second degree torsion equation are believed to be unimportant (see ref. 3), and are thus discarded. The well known tennis racquet effect term appears in the torsion equation as $m\Omega^2\phi \cos^2 \beta_{pc}(k_{m2}^2 - k_{m1}^2) \cos 2\theta$, while the tension-torsion coupling term appears in $[EAk_A^2 u'(\theta_{pt}' + \phi')]'$. The extensional degree of freedom in the present equations has been discarded, since it has been established in reference 11 that the effect of the extensional coupling on vibration and stability characteristics for practical blade configurations is insignificant. One can eliminate the extensional slope, u', by using equations (4) to (6). The effects of the tension-torsion and tennis racquet terms and the structural and inertial warping terms were discussed in detail in references 12 and 13 for uncoupled torsional vibration of pretwisted, rotating blades. In view of the discussion presented in these references, the inertial warping term is discarded and the structural warping effect terms is retained.

Defining the following parameters,

$$\bar{w} = w/L,\ \bar{v} = v/L,\ \eta = x/L,\ \tau = \Omega t,\ \bar{R} = R/L,\ \text{etc.,} \tag{8}$$

assuming solutions are separable in time and space, and making note of the following relations

$$\frac{d}{dx} = \frac{d\eta}{dx}\frac{d}{d\eta} = \frac{1}{L}\frac{d}{d\eta},\ \frac{d}{dt} = \Omega\frac{d}{d\tau}\ \text{etc.,} \tag{9}$$

one can write equations (1) to (3) in the following nondimensional forms:

$$
\begin{aligned}
&\ddot{\bar{w}} + \underline{2 \sin \beta_{pc} \dot{\bar{v}} - \bar{w} \sin^2 \beta_{pc}} + \left[2 \cos \beta_{pc} \dot{\phi} \left(mk_{m2}^2 \sin^2 \theta + mk_{m1}^2 \cos^2 \theta\right)\right] \Big/ mL^2 \\
&\underline{- \frac{1}{2} \sin \beta_{pc} \cos \beta_{pc} \int_0^{\eta} (\bar{v}'^2 + \bar{w}'^2)\, d\eta} \\
&- \cos^2 \beta_{pc} (\bar{w}'' Q - \bar{w}' s) \underline{- 2 \cos \beta_{pc} \left[\bar{w}'' \int_{\eta}^{1} \dot{\bar{v}}\, d\eta - \bar{w}' \dot{\bar{v}}\right]} \\
&\underline{+ \sin \beta_{pc} \cos \beta_{pc} \left[\bar{w}'' \int_{\eta}^{1} \bar{w}\, d\eta - \bar{w}' \bar{w}\right]} + \xi \bar{w}^{iv} \left(\cos^2 \theta + \frac{b^2}{d^2} \sin^2 \theta\right) \\
&+ \bar{w}''' (2\gamma\xi \sin 2\theta) \left(\frac{b^2}{d^2} - 1\right) + \bar{w}'' \, 2\gamma^2 \xi \cos 2\theta \left(\frac{b^2}{d^2} - 1\right) \\
&+ \xi \bar{v}^{iv} \left(\frac{b^2}{d^2} - 1\right) \sin \theta \cos \theta + \bar{v}''' (2\gamma\xi \cos 2\theta) \left(\frac{b^2}{d^2} - 1\right) \\
&- \bar{v}'' (2\gamma^2 \sin 2\theta) \left(\frac{b^2}{d^2} - 1\right) + \underline{\underline{\xi \left(\frac{b^2}{d^2} - 1\right) \Big\{ \bar{w}^{iv} \phi \sin 2\theta}} \\
&\underline{\underline{+ 2\bar{w}''' \phi' \sin 2\theta + \bar{w}'' \phi'' \sin 2\theta + 4\gamma \bar{w}''' \phi \cos 2\theta + 4\gamma \bar{w}'' \phi' \cos 2\theta}} \\
&\underline{\underline{- 4\gamma^2 \bar{w}'' \phi \sin 2\theta + \bar{v}^{iv} \phi \cos 2\theta + 2\bar{v}''' \phi' \cos 2\theta + \bar{v}'' \phi'' \cos 2\theta}} \\
&\underline{\underline{- 4\gamma \bar{v}''' \phi \sin 2\theta - 4\gamma \bar{v}'' \phi' \sin 2\theta - 4\gamma^2 \bar{v}'' \phi \cos 2\theta}} \Big\} \\
&- \frac{GJ}{m\Omega^2 L^4} \{\phi' \bar{v}''' + 2\phi'' \bar{v}'' + \phi''' \bar{v}'\} \\
&= - \eta \sin \beta_{pc} \cos \beta_{pc} - \frac{\gamma I_{\eta\eta}}{AL^2} \left(\frac{b^2}{d^2} - 1\right) \sin \beta_{pc} \cos \beta_{pc} \sin 2\theta \qquad (10)
\end{aligned}
$$

$$
\begin{aligned}
&\ddot{\bar{v}} - \underline{2 \sin \beta_{pc} \dot{\bar{w}}} - \bar{v} + \left[2 \cos \beta_{pc} \dot{\phi} \left(mk_{m2}^2 - mk_{m1}^2\right) \sin \theta \cos \theta\right]' / mL^2 \\
&\quad - \cos^2 \beta_{pc} \left(\bar{v}''Q - \bar{v}'S\right) - \underline{2 \cos \beta_{pc} \left[\bar{v}'' \int_{\eta}^{1} \dot{\bar{v}}\, d\eta - \bar{v}' \dot{\bar{v}}\right]} \\
&\quad \underline{- \cos \beta_{pc} \frac{d}{d\tau} \int_{0}^{\eta} \left(\bar{v}'^2 + \bar{w}'^2\right) d\eta + \sin \beta_{pc} \cos \beta_{pc} \left[\bar{v}'' \int_{\eta}^{1} \bar{w}\, d\eta - \bar{v}'\bar{w}\right]} \\
&\quad + \bar{w}^{iv} \xi \left(\frac{b^2}{d^2} - 1\right) \sin \theta \cos \theta + \bar{w}'''(2\gamma\xi \cos 2\theta) \left(\frac{b^2}{d^2} - 1\right) \\
&\quad - \bar{w}''\left(2\gamma^2\xi \sin 2\theta\right)\left(\frac{b^2}{d^2} - 1\right) + \bar{v}^{iv} \xi \left(\sin^2 \theta + \frac{b^2}{d^2} \cos^2 \theta\right) \\
&\quad - \bar{v}'''(2\gamma\xi \sin 2\theta) \left(\frac{b^2}{d^2} - 1\right) - \bar{v}''\left(2\gamma^2\xi \cos 2\theta\right)\left(\frac{b^2}{d^2} - 1\right) \\
&\quad + \underline{\frac{GJ}{m\Omega^2 L^4} \left(\phi''\bar{w}'' + \phi'\bar{w}'''\right)} + \underline{\underline{\xi \left(\frac{b^2}{d^2} - 1\right) \left\{\bar{w}^{iv} \phi \cos 2\theta\right.}} \\
&\quad \underline{\underline{+ 2\bar{w}'''\phi' \cos 2\theta + \bar{w}''\phi'' \cos 2\theta - 4\gamma\bar{w}'''\phi \sin 2\theta - 4\gamma\bar{w}''\phi' \sin 2\theta}} \\
&\quad \underline{\underline{- 4\gamma^2 \bar{w}''\phi \cos 2\theta - \bar{v}^{iv}\phi \sin 2\theta + 2\bar{v}'''\phi' \sin 2\theta + \bar{v}''\phi'' \sin 2\theta}} \\
&\quad \underline{\underline{\left. + 4\gamma\bar{v}'''\phi \cos 2\theta + 4\gamma\bar{v}''\phi' \cos 2\theta - 4\gamma^2\bar{v}'' \sin 2\theta\right\}}} \\
&\quad = - \sin \beta_{pc} \cos \beta_{pc} \left(\frac{\gamma I_{\eta\eta}}{AL^2}\right) \cos 2\theta \qquad (11)
\end{aligned}
$$

$$
\begin{aligned}
&\ddot{\phi} + f_1 \cos^2 \beta_{pc}(\phi \cos 2\theta) + 2f_1 \cos \beta_{pc}\dot{\bar{v}}' \sin \theta \cos \theta + 2 \cos \beta_{pc}\dot{\bar{w}}' \Big(f_2 \sin^2 \theta \\
&+ f_3 \cos^2\theta\Big) + f_4\phi^{iv} + \sin \beta_{pc} \cos \beta_{pc} \left\{\phi'' \int_\eta^1 \bar{w}\, d\eta - \phi'\bar{w} - \gamma\bar{w}\right\} \\
&- \cos^2 \beta_{pc}(\phi''Q - \phi'S) - 2 \cos \beta_{pc}\left(\phi'' \int_\eta^1 \dot{\bar{v}}\, d\eta - \phi'\dot{\bar{v}} - \gamma\dot{\bar{v}}\right) \\
&+ f_5(2\gamma\phi'\phi'' + \gamma^2\phi'') - f_6\phi'' - f_7\phi'' + f_7(\bar{v}'\bar{w}''' + \bar{v}''\bar{w}'') \\
&+ f_8\cos^2 \beta_{pc}\phi'' - 2\gamma f_8 \sin \beta_{pc} \cos \beta_{pc}\bar{w}'' - f_1 \sin \beta_{pc} \cos \beta_{pc}\bar{v}' \cos 2\theta \\
&- f_1 \sin \beta_{pc} \cos \beta_{pc}\bar{w}' \sin 2\theta + f_9\bar{v}''\bar{w}'' \cos 2\theta + f_9(\bar{w}''^2 - \bar{v}''^2) \sin \theta \cos \theta \\
&= - f_1 \cos^2 \beta_{pc} \sin \theta \cos \theta - \gamma S \cos^2 \beta_{pc}
\end{aligned}
\tag{12}
$$

where

$$Q = \bar{R}(1 - \eta) + 0.5(1 - \eta^2),\quad S = (\bar{R} + \eta),$$

$$f_1 = \frac{k_{m2}^2 - k_{m1}^2}{k_m^2} = \frac{b^2 - d^2}{b^2 + d^2},\quad f_2 = \frac{k_{m2}^2}{k_m^2} = \frac{b^2}{b^2 + d^2},$$

$$f_3 = \frac{k_{m1}^2}{k_m^2} = \frac{d^2}{b^2 + d^2},\quad f_4 = \frac{EC_1}{m\Omega^2 k_m^2 L^4} = \frac{Eb^2d^2}{12\rho\Omega^2 L^4(b^2 + d^2)};$$

$$f_5 = \frac{EAk_A^4}{m\Omega^2 k_m^2 L^4} = \frac{E(b^2 + d^2)}{12\rho L^4\Omega^2},\quad f_6 = \frac{EB_1\theta_{pt}'^2}{m\Omega^2 k_m^2 L^2} = \frac{E\gamma^2 b^4}{15\rho\Omega^2 L^4(b^2 + d^2)};$$

$$f_7 = \frac{GJ}{m\Omega^2 k_m^2 L^2} = \frac{4Gt^2}{\rho\Omega^2 L^2(b^2 + d^2)},\quad f_8 = \frac{mk_\lambda^4}{mk_m^2 L^2} = \frac{b^2t^2}{12L^2(b^2 + d^2)},$$

$$f_9 = \frac{E(I_{\xi\xi} - I_{\eta\eta})}{\rho\Omega^2 L^2 (I_{\xi\xi} + I_{\eta\eta})} = \frac{E(b^2 - d^2)}{\rho\Omega^2 L^2 (b^2 + d^2)}, \quad f_{10} = \frac{GJ}{m\Omega^2 L^4},$$

$$f_{11} = \xi\left(\frac{b^2}{d^2} - 1\right), \quad \xi = \frac{EI_{\eta\eta}}{\rho A L^4 \Omega^2}, \quad \theta = \alpha + \gamma\eta, \quad \theta_{pt} = \frac{\gamma x}{L} = \gamma\eta,$$

$$\bar{w}' = \frac{d}{d\eta}(\bar{w}) \quad \text{and} \quad \dot{\bar{w}} = \frac{d}{d\tau}(\bar{w}) \; . \; . \; . \; . \; . \qquad (13)$$

Before discussing the method of solution, it is worthwhile to point out the various important linear and nonlinear terms in the present equations. In equations (10) and (11), certain linear and nonlinear terms are underlined once. These terms constitute the linear and nonlinear Coriolis force terms and nonlinear terms arising from the foreshortening, (u_F), and tension terms, $(Tw')'$ and $(Tv')'$. Individual and collective effects of these important terms were assessed in references 10 and 11. It was shown in these references that the linear and nonlinear Coriolis effect terms significantly affect the onset of instability for large preconed thick blades and thus they must be retained in analyzing blades having moderate to large thickness ratios. It was also shown that the nonlinear terms in the coupled bending-bending equations which vanish for zero precone are extremely important. These terms can produce significant frequency changes (of the order of 20 percent increase in the fundamental mode frequency for a 45° preconed thin or thick blade rotating at a speed equal to the fundamental frequency of the same blade). Next, the Coriolis effect terms due to torsional coupling in the bending equations and the flexural coupling in the torsion equation are addressed. Referring to equations (10) and (11), one can find the Coriolis effect terms $[2 \cos \beta_{pc}\dot{\phi}(mk_{m2}^2 \sin^2 \theta + mk_{m1}^2 \cos^2 \theta)/mL^2]'$ and $[2 \cos \beta_{pc}\dot{\phi}(mk_{m2}^2 - mk_{m1}^2) \sin \theta \cos \theta/mL^2]'$. The corresponding terms in the torsion equation are $2f_1\dot{\bar{v}}' \sin \theta \cos \theta \cos \beta_{pc} + 2 \cos \beta_{pc}\dot{\bar{w}}'(f_2 \sin^2 \theta + f_3 \cos^2 \theta)$. It may be noted that the linear Coriolis forces, $2 \sin \beta_{pc}\dot{\bar{v}}$ and $-2 \sin \beta_{pc}\dot{\bar{w}}$, in the two bending equations indicate skew symmetry of the gyroscopic matrix. One may thus consider that inclusion of torsional degree of freedom does not alter this nature of the gyroscopic matrix provided that an appropriate sign change is made in the torsion equation throughout. Keeping in view the ordering scheme followed, the bending equations should contain terms of order $O(\epsilon^2)$ in the inertial terms. Consequently, the Coriolis effect terms in the bending equations which are associated with the torsion variable $\dot{\phi}$ should be discarded. To preserve the skew symmetric nature of the gryoscopic matrix in linear Coriolis force terms, one must discard the corresponding Coriolis force terms in the torsion equation also. In the following, we maintain this consistency and disregard the aforementioned Coriolis effect terms associated with $\dot{\phi}$ in the bending equations (10) and (11) and all the Coriolis force terms in the torsion equation.

Finally, the twice underlined terms in the bending equations are the nonlinear terms arising from torsional coupling with the bending motions (pitch-flap and pitch-lag couplings). The corresponding terms in the torsion equation are shown by underscoring them thrice. These terms were first discussed by Mil et al. (ref. 14) and subsequently by others. From the present equations, it can be seen that these terms are premultiplied by the rotational parameter ξ and square of thickness ratio factor, $(b^2/d^2 - 1)$. For thin blades, the

flatwise steady state deflection, $\overline{w}$, will become significant with increasing speeds and makes these terms quite significant in the perturbation equations. Furthermore, these effects are aggravated due to the coefficient $(b^2/d^2 - 1)$ as the thickness ratio (d/b) becomes smaller. Thus, one may anticipate a significant influence of these terms on the vibration and stability behavior of thin blades subjected to large rotational speeds. The terms shown by the dashed underlining are associated with the torsional rigidity, GJ, and the terms shown by the double dashed underlining arise due to tension effects. It will be shown that these terms are not as significant as the aforementioned nonlinear terms.

The coupled bending-bending-torsion equations are solved by the Galerkin method by expanding the dimensionless deflections in terms of a series of generalized coordinates and mode shape functions as follows:

$$\bar{w} = \sum_j (w_{0j} + \Delta w_j(\tau))\psi_j(\eta) \tag{14}$$

$$\bar{v} = \sum_j (v_{0j} + \Delta v_j(\tau))\psi_j(\eta) \tag{15}$$

$$\phi = \sum_j (\phi_{0j} + \Delta\phi_j(\tau))\theta_j(\eta) \tag{16}$$

where

$$\psi_j(\eta) = \cosh(\beta_j\eta) - \cos(\beta_j\eta) - \alpha_j[\sin(\beta_j\eta) - \sin(\beta_j\eta)] \tag{17}$$

$$\theta_j(\eta) = 2\sin(\gamma_j\eta) \tag{18}$$

$$\gamma_j = \pi(j - \frac{1}{2}) \tag{19}$$

Equations (17) and (18) represent the nonrotating normal modes for a cantilevered beam fixed at $\eta = 0$ and free at $\eta = 1$. The values of β_j are taken from reference 15. It may be noted here that sinusoidal mode shape assumed for the torsional degree of freedom is not compatible with the boundary conditions when warping is included. However, the effect of warping is not significant for large aspect ratio blades ($L/b \geq 6$ (ref. 13)). Thus, the mode shape assumed here should produce satisfactory results for blades with moderate aspect ratios. The quantities w_{0j}, v_{0j} and ϕ_{0j} are the equilibrium quantities while Δw_j, Δv_j and $\Delta\phi_j$ are the perturbation quantitites in the generalized coordinates.

Proceeding as in reference 11, one can apply the Galerkin process for the solution of the nonlinear steady state equations and the linearized perturbation equations (expressed in terms of the equilibrium generalized coordinates) which define the blade motion about the equilibrium operating condition.

The steady state equilibrium equations, and the linear perturbation equations are written in the following forms for a solution with n normal modes assumed for each independent variable:

$$[\underset{\sim}{L} + \underset{\sim}{NL}]\ \{x_o\} = \{B\} \tag{20}$$

$$[\underset{\sim}{M}]\ \{\ddot{x}\} + [\underset{\sim}{C}]\ \{\dot{x}\} + [\underset{\sim}{K}]\ \{x\} = 0 \tag{21}$$

where

$$\{x_o\} = \{w_{o1}, w_{o2}, \ldots, w_{on}, v_{o1}, v_{o2}, \ldots, v_{on}, \phi_{o1}, \phi_{o2}, \ldots, \phi_{on}\}^T \tag{22}$$

$$\{x\} = \{\Delta w_1, \Delta w_2, \ldots, \Delta w_n, \Delta v_1, \Delta v_2, \ldots, \Delta v_n, \Delta\phi_1, \Delta\phi_2, \ldots, \Delta\phi_n\}^T \tag{23}$$

with $\underset{\sim}{L}$, $\underset{\sim}{LN}$ being the linear and nonlinear parts of the equilibrium equations, and $\underset{\sim}{M}$, $\underset{\sim}{C}$, and $\underset{\sim}{K}$ being the mass, Coriolis and stiffness matrices respectively. Elements of those matrices are presented in appendix A.

RESULTS AND DISCUSSION

The nonlinear, steady state, equilibrium equations (20), and the eigenvalue problem that results from the transformation of equation (21) were solved by using computer programs developed in FORTRAN language. Integrations are performed on the computer using a 15 point Gaussian quadrature formula. The general computer program developed for the solution of equation (21) gives the natural frequencies per unit rotational speed, (p/Ω). In the presence of Coriolis forces, the frequencies will occur in pairs of purely imaginary quantities for a conservative system. In the absence of Coriolis effects, the frequency equation (21) reduces to a standard eigenvalue problem the eigenvalues of which are real quantities, (p^2/Ω^2). Specialized cases were solved by modifying the general computer program. Parametric studies were conducted for thickness ratios (d/b) ranging from 0.05 (representing approximately an advanced turboprop blade) to 0.25 (representing approximately a conventional propeller blade) for various precone angles, pretwists, setting angles and rotational speeds. The disc radius is assumed to be zero in most of the calculations except for cases corresponding to a test configuration developed at the NASA Lewis (ref. 16). Results were also generated from the finite element code, MSC/NASTRAN, using 250 or 500 CQUAD4 elements for the purpose of comparisons with present theoretical results. It should be noted here that the MSC/NASTRAN calculations ignore the Coriolis effects although there is no restriction on the degree of geometric nonlinear terms. All these results are presented and discussed in what follows.

Convergence

The convergence of the solutions produced by the Galerkin method with various numbers of nonrotating normal modes in the coordinate functions is illustrated in table I. The blade considered for this convergence study has a precone of 15°, pretwist of 30° at its tip, and a thickness ratio of 0.05. The blade chord at the root is set perpendicular to the axis of rotation (α = 0°) and the blade rotational speed is one-half of the fundamental mode

frequency of the same nonrotating blade with zero pretwist and zero precone (Ω/ω_1 = 0.50). The frequency ratios (p/λ) shown in table I are representative of the convergence trend that one might expect for a general case of pretwisted rotating blade when geometric nonlinearities up to second degree and Coriolis effects are included in the analysis. For the purpose of comparison of the present beam theory results, and to provide a measure of accuracy of the present beam theory formulation, the results produced by MSC/NASTRAN by using 500 CQUAD4 elements are also included in this table. The convergence pattern of the components of steady state, dimensionless, tip deflections are shown in table II for this blade as obtained from the Galerkin method calculations together with those produced by MSC/NASTRAN.

From the convergence pattern of the frequency ratios presented in table I, it can be seen that a five mode solution produces the lowest six coupled bending-bending-torsion frequencies that are in reasonable agreement with the corresponding values produced by MSC/NASTRAN. Furthermore, the steady state deflections produced by the present beam theory calculations with a five mode solution agree quite closely with those from MSC/NASTRAN. Among the several factors unknown so far, the sinusoidal mode functions used for torsional deformation instead of hyperbolic functions may perhaps be responsible for the oscillatory convergence trend observed for the frequencies and steady state deflections shown in tables I and II as the number of nonrotating normal modes in the assumed solutions are increased. It emerges clearly, however, that the convergence of higher mode frequencies to accurate values can be accomplished by increasing the number of modes in the solution, and that accuracies of practical interest can be achieved from the present theoretical formulation. Finally, the close agreement of the present theoretical results, including Coriolis effects, with the MSC/NASTRAN results, that ignore the Coriolis effects, substantiate the conclusion reached by the present authors in reference 11 that Coriolis effects can safely be ignored for thin blades.

Comparison with Experimental Results

In order to verify the present theoretical development of the equations of motion, a typical set of results were obtained for rotating, preconed, untwisted blade cases corresponding to those obtained from the NASA Lewis spin test rig (ref. 16). The test rig is capable of accommodating bladed rotors up to 51 cm (20 in.) in diameter, which can be spun to 16 000 rpm. A rotor capable of holding two blades with adjustable sweep (precone) and setting angles, was designed for this spin rig. Tests were conducted for nonrotating, steel, flat plates having an aspect ratio, L/b, of 3 and thickness ratio, d/b, of 0.05. Frequencies of the lowest five modes as given by the static spin rig tests were 94.2, 572, 586, (1643.5±11.5) and 1795 Hz respectively. Results obtained from the holography tests were respectively 93.0, 572, 586, 1628, and 1793 for the lowest five mode frequencies. Of these frequencies, the first two correspond to the fundamental bending and torsion modes of the flat plate respectively.

In order to match these frequencies from theoretical considerations, the elastic moduli were determined from standard relations. A value of 0.283 lb/in^3 was chosen for the mass density. The effective root distance from the center of rotation of the spin rig varies slightly with the precone. For precones of zero, 22.5° and 45°, the effective root distances were 4.0, 3.952, and 3.816 in., respectively. Using these geometric and physical properties,

numerical results were generated for various setting angles, precones, and rotational speeds. Corresponding results obtained from the test rig are compared to the present theoretical results in table III.

An examination of these results, presented in table III, indicates that there is a reasonable agreement between the theoretical and experimental results for all the cases considered. Furthermore, the trends shown by the theoretical and experimental results are consistent. From the comparison of the theoretical and experimental results shown in table III (of the order of ± 6 percent difference in most of the cases considered), and from the close agreement between the theoretical results and NASTRAN generated results presented in tables I and II, it is concluded that the present theoretical formulation is accurate, and that it is capable of producing accurate results for the parameters considered here.

Vibration and Stability of Preconed, Rotating Blades

In order to determine the individual and combined influence of pretwist, precone, Coriolis forces, second degree geometric nonlinearities and rotation on the coupled frequencies or stability boundaries, parametrics studies were conducted for various thickness ratio blade cases. A typical set of such results are shown in table IV. Also included in this table are the results produced by MSC/NASTRAN. Figure 2 shows a further comparison of frequency ratios obtained from the present beam theory and from MSC/NASTRAN for typical precones and thickness ratio cases. A comparison of these results indicates that there is a good agreement between the present theoretical results and MSC/NASTRAN results for blade cases having moderate thickness ratios ($d/b \geq 0.10$), moderate precones ($\beta_{pc} = 15°$) and for a wide range of rotational speeds (Ω/ω_1 up to 2.0). This trend of close agreement between the beam theory results including second degree geometric nonlinearities and those from MSC/NASTRAN continues for blades with increasing thickness ratios for a wider range of precone angles and rotational speeds (see fig. 2(b)). In the absence of precone, the present beam theory results agree very closely with MSC/NASTRAN results for all thickness ratios, (see fig. 2(a)), over a wide range of rotational speeds. However, when the thickness ratio is decreased, the agreement between the beam theory results and MSC NASTRAN results is found to be close for low rotational speeds (up to about $\Omega/\omega_1 = 0.5$ to 0.8) only (see fig. 2(c) and table IV).

From the parametric results generated, it was found that the present beam theory predicts torsional instability for thin blades ($d/b = 0.05$ or 0.06) at lower rotational speeds than does MSC/NASTRAN. This trend can be verified from the results presented in table IV for the case of a thin blade ($d/b = 0.05$) having 30° pretwist and 15° precone. For this particular blade configuration, the beam theory results are in close agreement with those of MSC/NASTRAN for a rotational speed parameter value of $\Omega/\omega_1 = 0.5$. However, when the rotational speed is increased, the torsional frequency predicted by the beam theory was found to be unstable, although the corresponding one from the MSC/NASTRAN calculation was stable. Similar trends were observed for this blade case even in the absence of pretwist (see fig. 2(c)). Furthermore, a comparison of the results presented in table IV for the present blade case with $\Omega/\omega_1 = 1.0$ indicates that the flexural frequencies predicted by the beam theory and NASTRAN calculations are still in very close agreement. Similar trends of

instability could also be found for blades of the same thickness ratio, rotational speed and pretwist but larger values of precones.

From the comparison of the results presented in table IV, the following observations are made:

(1) For blades of moderate thickness ratios (d/b of the order of 0.10 and greater), for moderate precones (β_{pc} of the order of up to 15°), and for rotational speeds of up to $\Omega/\omega_1 = 2.0$, inclusion of geometric nonlinearities up through second degree only appears to be adequate for a fair prediction of the blade frequencies. Thus, the present second degree equations appear to be adequate for application to helicopter blade vibration analysis.

(2) The effect of Coriolis forces on the frequencies of rotating preconed blades is insignificant for low thickness ratio blade cases, but could become significant for high thickness ratio blade cases (refer to the results presented in table IV). Conclusions concerning the linear and nonlinear Coriolis forces on the frequencies of rotating blades that were presented in reference 11 are valid here also.

(3) Thin blades possessing large precones and subjected to considerable rotational speeds exhibit torsional divergence at a much earlier rotational speed when the present beam theory is used than is the case when MSC/NASTRAN is used.

In order to acquire further insight into the torsional instability of thin blades, results produced by the present beam theory and MSC/NASTRAN are presented in table V for an untwisted, 15° preconed, thin blade ($d/b = 0.05$) for various rotational speeds. To facilitate a clearer understanding, the frequencies are listed in a columnwise fashion, each column corresponding to one of the bending modes (F1, F2, F3, F4) in the flatwise direction, the torsion mode (T1) or the edgewise bending mode (S1) respectively. Also included are the dimensionless steady state tip deflections $(\overline{w},\overline{v},\phi)$ in the last three columns of this table. An examination of the results presented in table V indicates that for all rotational speeds considered, the flatwise steady state deflection, $\overline{w}$, is the most significant one while the edgewise and torsional deformations are insignificant, as expected for the untwisted blade. Furthermore, the steady state deflections produced by the present beam theory are in excellent agreement with those from MSC/NASTRAN. Since the flatwise deflection is the only significant one that can contribute to the nonlinear terms in the perturbation solution, corresponding terms in the torsional equations causing instability could easily be identified. For the system to be unstable, the off-diagonal terms in the stiffness matrix should become large and negative. An examination of the stiffness matrix, $[\underset{\sim}{K}]$, for the perturbation solution, presented in appendix A indicates that the nonlinear terms $T8_{ijk}$, $T9_{ijk}$ and $T10_{ijk}$ are associated with the steady state equilibrium coordinates w_{ok}, and that these terms arise from the terms discussed by Mil et al. (ref. 14). To verify this, results for same blade configuration presented in table V are reproduced in table VI, but with the Mil's terms discarded. From table VI, it can be seen that the instabilities predicted by the present beam theory, shown in table V, vanish once the Mil's terms are discarded. However, the coupling trend between the fundamental torsional mode (T1) and the fundamental edgewise mode (S1), which now becomes evident by a mutual comparison of the results presented in tables V and VI [which decreases the lower uncoupled

frequency and increases the higher uncoupled frequency with increasing rotational speeds] is also absent. Further, the present beam theory frequencies are more closely in agreement with those from MSC/NASTRAN when the Mil's terms are present than when they are absent, in so far as stable configurations are compared. Thus, it can be concluded that the Mil's terms are necessary for a reasonable prediction of the coupled bending-torsional frequencies, however, they also can cause torsional divergence for thin blades at larger precones and rotational speeds. It appears, then, that the level of approximation used for the Mil's terms may not be adequate, and inclusion of the complete set of Mil's terms, (presently truncated in accordance with the ordering scheme or degree of geometric nonlinearity retained in the equations), may improve the present theoretical prediction of instability. These aspects are yet to be investigated.

Finally, the effect of various nonlinear terms on the coupled bending-bending-torsion frequencies of a particular blade with a 15° or 45° precone are presented in table VII. For assessing the individual effect of each key nonlinear terms, solution of the present nonlinear equations is accomplished by retaining all nonlinear terms other than the one key element being addressed. Thus, in table VII, results under the column with $T5_{ijk} = T6_{ijk} = 0$ represent nonlinear frequencies obtained by discarding the nonlinear terms arising from the tension effects in the torsion equation, results under the column with $T1_{ijk} = T4_{ijk} = T8_{ijk} = 0$ correspond to elimination of those nonlinear terms associated with GJ in the two bending equations together with $GJ(v'w'')'$ in the torsion equation, and those under the column $T3_{ijk} = T9_{ijk} = 0$ ($T2_{ijk} = T10_{ijk} = 0$ for $\alpha = 0$) correspond to elimination of the Mil's terms. Further, when A_{ijk} is set to zero, the foreshortening effects are ignored, while $D_{ijk} = E_{ijk} = 0$ neglects the nonlinear terms arising from $(Tw')'$ and $(Tv')'$. From the results presented in table VII, and by comparing them with those presented in table IV one can observe that:

(1) The affect of the terms $(\phi'v'GJ)''$ and $(\phi''w''GJ)'$ in the two bending equations (1) and (2) and the corresponding term $(GJv'w'')'$ in the torsion equation (3) is negligible on the coupled bending-bending-torsional frequencies. These terms can therefore be neglected.

(2) The affect of nonlinear terms arising from the tension coupling in the torsion equation is also negligible on the coupled frequencies.

(3) The Mil's terms are extremely important in bringing in the bending-torsional coupling, and can also cause torsional divergence for thin blades. Further study with a careful consideration of these terms in their complete form is necessary.

(4) Compared to the Mil's terms just discussed, all other nonlinear terms that result due to the torsional coupling in the bending-torsion equations appear to be unimportant.

(5) Effects of the nonlinear terms arising due to foreshortening, tension coupling with flexural motions, [$(Tv')'$ and $(Tw')'$], and Coriolis effects were discussed in reference 11 in detail. These terms are extremely important and must be retained in the equations. Conclusions concerning these terms as drawn in reference 11 are valid even in the presence of torsional coupling addressed in the present work.

CONCLUDING REMARKS

The coupled bending-bending-torsion equations of dynamic motion of rotating linearly pretwisted and large preconed blades of symmetric cross section including second degree geometric nonlinearities and Coriolis effects are derived. These equations are solved by using the Galerkin method and a linear perturbation procedure. Natural frequencies and steady state deflections produced by the solution of the present set of nonlinear equations are compared to those produced by MSC/NASTRAN calculations and also to those from experiment. Close agreement of the present theoretical results with those from other methods establishes the accuracy of the equations developed and the method of solution adopted. Parameter limits within which the second degree geometric nonlinearities are adequate for a fair prediction of natural frequencies and steady state deflections are established. The following specific conclusions have emerged from the present investigation.

(1) For blades of moderate thickness ratios $(d/b \geq 0.10)$ and moderate precones $(\beta_{pc} \leq 15°)$, inclusion of geometric nonlinearities up through second degree appears to be adequate for a fair prediction of the coupled frequencies and steady state deflections.

(2) The present nonlinear equations indicate torsional divergence at lower rotational speeds when the thickness ratio is decreased and the blade precone is increased than do the finite element calculations. The nonlinear terms contributing to the coupling between bending and torsional motions, often referred to as kinematic pitch coupling terms and first discussed by Mil et al. (ref. 14) were found to be responsible for this torsional divergence. These terms are extremely important in producing the accurate coupling between the bending and torsional frequencies. Inclusion of a complete set of these terms (presently appearing in the equations in a truncated form) may lead to a satisfactory stability calculations.

(3) The affect of linear and nonlinear Coriolis forces on the coupled frequencies of thin blades is found to be negligible. The Coriolis force terms can therefore be safely ignored in analyzing advanced turboprop type blade configurations. However, the Coriolis effects must be retained in analyzing thick blades, as discussed in reference 11.

(4) The affect of nonlinear terms arising from the tension coupling in the torsion equation, and the terms $(GJ\phi'v')''$, $(GJ\phi''w'')'$ and $(GJv'w'')'$ appearing respectively in the flatwise, edgewise and torsion equations, is found to be negligible on the coupled frequencies and steady state deflections for preconed rotating blades.

APPENDIX A:

THE GALERKIN INTEGRALS AND MODAL EQUATIONS

The various integrals arising from the Galerkin process are defined below, and these are used in representing the modal equations in matrix forms subsequently:

$$\delta_{ij} = \int_0^1 \psi_i \psi_j \, d\eta = \int_0^1 \theta_i \theta_j \, d\eta = \begin{matrix} 0 \\ 1 \end{matrix} \left\{ \begin{matrix} i \neq j \\ i = j \end{matrix} \right.$$

$$A_{ijk} = \int_0^1 \psi_i \int_0^\eta \psi_j'(\bar{x}) \psi_k'(\bar{x}) \, d\bar{x} \, d\eta$$

$$B_{ij} = \int_0^1 \psi_i \psi_j'' Q \, d\eta$$

$$C_{ij} = \int_0^1 \psi_i \psi_j' S \, d\eta$$

$$D_{ijk} = \int_0^1 \psi_i \psi_j'' \int_\eta^1 \psi_k(\bar{x}) \, d\bar{x} \, d\eta$$

$$E_{ijk} = \int_0^1 \psi_i \psi_j'' \psi_k \, d\eta$$

$$F_{ij} = \int_0^1 \psi_i \psi_j^{iv} \left(\cos^2 \theta + \frac{b^2}{d^2} \sin^2 \theta \right) d\eta$$

$$G_{ij} = \int_0^1 \psi_i \psi_j''' \sin 2\theta \, d\eta$$

$$H_{ij} = \int_0^1 \psi_i \psi_j'' \cos 2\theta \, d\eta$$

$$I_{ij} = \int_0^1 \psi_i \psi_j^{iv} \sin 2\theta \, d\eta$$

$$J_{ij} = \int_0^1 \psi_i \psi_j''' \cos 2\theta \, d\eta$$

$$K_{ij} = \int_0^1 \psi_i \psi_j'' \sin 2\theta \, d\eta$$

$$L_i = \int_0^1 \psi_i \eta \, d\eta$$

$$M_{ij} = \int_0^1 \psi_i \psi_j^{iv} \left(\sin^2 \theta + \frac{b^2}{d^2} \cos^2 \theta \right) d\eta$$

$$N_{ij} = \int_0^1 \psi_i \psi_j'' \, d\eta$$

$$O_{ij} = \int_0^1 \psi_i \theta_j \, d\eta$$

$$R_{ij} = \int_0^1 \theta_i \theta_j'' \, d\eta$$

$$S_i = \int_0^1 \theta_i \eta \, d\eta$$

$$u_i = \int_0^1 \psi_i \sin 2\theta \, d\eta$$

$$v_i = \int_0^1 \psi_i \cos 2\theta \, d\eta$$

$$T1_{ijk} = \int_0^1 \psi_i \left(\theta_j' \psi_k''' + 2\theta_j'' \psi_k'' + \theta_j''' \psi_k' \right) d\eta$$

$$T2_{ijk} = \int_0^1 \psi_i \Big[\theta_j \psi^{iv} \sin 2\theta + 2\theta_j' \psi_k''' \sin 2\theta + \theta_j'' \psi_k'' \sin 2\theta + 4\gamma \theta_j \psi_k''' \cos 2\theta + 4\gamma \theta_j' \psi_k'' \cos 2\theta - 4\gamma^2 \theta_j \psi_k'' \sin 2\theta \Big] d\eta$$

$$T3_{ijk} = \int_0^1 \psi_i \Big[\theta_j \psi^{iv} \cos 2\theta + 2\theta_j' \psi_k''' \cos 2\theta + \theta_j'' \psi_k'' \cos 2\theta - 4\gamma \theta_j \psi_k''' \sin 2\theta - 4\gamma \theta_j' \psi_k'' \sin 2\theta - 4\gamma^2 \theta_j \psi_k'' \cos 2\theta \Big] d\eta$$

$$T4_{ijk} = \int_0^1 \psi_i \left(\theta_j''\psi_k'' + \theta_j'\psi_k'''\right) d\eta$$

$$T5_{ijk} = \int_0^1 \theta_i\theta_j'' \int_\eta^1 \psi_k(\bar{x})\, d\bar{x}\, d\eta$$

$$T6_{ijk} = \int_0^1 \theta_i\theta_j'\, \psi_k\, d\eta$$

$$T7_{ijk} = \int_0^1 \theta_i\theta_j'\, \theta_k''\, d\eta$$

$$T8_{ijk} = \int_0^1 \theta_i \left(\psi_j'\psi_k''' + \psi_j''\psi_k''\right) d\eta$$

$$T9_{ijk} = \int_0^1 \theta_i\psi_j''\psi_k'' \cos 2\theta\, d\eta$$

$$T10_{ijk} = \int_0^1 \theta_i\psi_j''\psi_k'' \sin\theta \cos\theta\, d\eta$$

$$S1_{ij} = \int_0^1 \theta_i\theta_j \cos 2\theta\, d\eta$$

$$S2_{ij} = \int_0^1 \theta_i\psi_j' \sin\theta \cos\theta\, d\eta$$

$$S3_{ij} = \int_0^1 \theta_i\psi_j' \left(f_2 \sin^2\theta + f_3 \cos^2\theta\right) d\eta$$

$$S4_{ij} = \int_0^1 \theta_i\theta_j^{iv}\, d\eta$$

$$S5_{ij} = \int_0^1 \theta_i \left(\theta_j''Q - \theta_j'S\right) d\eta$$

$$S6_{ij} = \int_0^1 \theta_i\psi_j''\, d\eta$$

$$S7_{ij} = \int_0^1 \theta_i \psi_j' \cos 2\theta \, d\eta$$

$$S8_i = \int_0^1 \theta_i \sin\theta \cos\theta \, d\eta$$

The linear and nonlinear parts of the steady state equilibrium equations are presented below in the matrix form, $[\underset{\sim}{L} + \underset{\sim}{NL}]\{X_0\} = \{B\}$

$$
\left[\begin{array}{l|l|l}
\begin{array}{l}
\sin^2\beta_{Pc}\delta_{ij} - \frac{1}{2}\sin\beta_{Pc}\cos\beta_{Pc}\sum_k w_{ok}A_{ijk} \\
- \cos^2\beta_{Pc}(B_{ij} - C_{ij}) + \sin\beta_{Pc}\cos\beta_{Pc} \times \\
\sum_k \left\{ w_{ok}D_{ijk} - w_{ok}E_{ijk} \right\} \\
+ \xi\left[F_{ij} + 2\gamma\left(\frac{b^2}{d^2} - 1\right) G_{ij} + \right. \\
\left. 2\gamma^2\left(\frac{b^2}{d^2} - 1\right) H_{ij}\right]
\end{array}
&
\begin{array}{l}
- \frac{1}{2}\sin\beta_{Pc}\cos\beta_{Pc}\sum_k v_{ok}A_{ijk} + \\
\xi\left(\frac{b^2}{d^2} - 1\right)\left\{\frac{1}{2} I_{ij} + 2\gamma J_{ij} - 2\gamma^2 K_{ij}\right\}
\end{array}
&
\begin{array}{l}
- f_{10}\sum_k v_{ok}T1_{ijk} \\
+ f_{11}\sum_k w_{ok}T2_{ijk} \\
+ f_{11}\sum_k v_{ok}T3_{ijk}
\end{array}
\\ \hline
\begin{array}{l}
\cos\beta_{Pc}\sin\beta_{Pc}\sum_k (v_{ok}D_{ikj} - v_{ok}E_{ikj}) \\
+ \xi\left(\frac{b^2}{d^2} - 1\right)\left\{\frac{1}{2} I_{ij} + 2\gamma J_{ij} - 2\gamma^2 K_{ij}\right\}
\end{array}
&
\begin{array}{l}
- \delta_{ij} - \cos^2\beta_{Pc}(B_{ij} - C_{ij}) + \\
\xi\left\{M_{ij} - 2\gamma\left(\frac{b^2}{d^2} - 1\right)\left[G_{ij} - \right.\right. \\
\left.\left. - 2\gamma^2\left(\frac{b^2}{d^2} - 1\right)H_{ij}\right]\right\}
\end{array}
&
\begin{array}{l}
f_{10}\sum_k w_{ok}T4_{ijk} \\
+ f_{11}\sum_k w_{ok}T3_{ijk} \\
- f_{11}\sum_k v_{ok}T2_{ijk}
\end{array}
\\ \hline
\begin{array}{l}
- \gamma\sin\beta_{Pc}\cos\beta_{Pc}O_{ji} \\
- 2\gamma f_8\sin\beta_{Pc}\cos\beta_{Pc}S6_{ij} \\
- 2f_1\sin\beta_{Pc}\cos\beta_{Pc}S2_{ij} \\
+ \sin\beta_{Pc}\cos\beta_{Pc}\sum_k \varphi_{ok}(T5_{ikj} - T6_{ikj}) \\
+ f_9\sum_k w_{ok}T10_{ijk}
\end{array}
&
\begin{array}{l}
- f_1\sin\beta_{Pc}\cos\beta_{Pc}S7_{ij} \\
+ f_7\sum_k w_{ok}T8_{ijk} \\
+ f_9\sum_k w_{ok}T9_{ijk} \\
- f_9\sum_k v_{ok}T10_{ijk}
\end{array}
&
\begin{array}{l}
f_1\cos^2\beta_{Pc}S1_{ij} \\
+ f_4 S4_{ij} \\
- \cos^2\beta_{Pc}S5_{ij} \\
+ (\gamma^2 f_5 - f_6 - f_7 \\
+ f_8\cos^2\beta_{Pc})R_{ij} \\
- 2\gamma f_5\sum_k \varphi_{ok}T7_{ijk}
\end{array}
\end{array}\right]
\left\{\begin{array}{c}
w_{oj} \\ \hline v_{oj} \\ \hline \varphi_{oj}
\end{array}\right\}
=
\left\{\begin{array}{l}
\begin{array}{l}
- \sin\beta_{Pc}\cos\beta_{Pc}L_i \\
- \left(\frac{\gamma I_{\eta\eta}}{AL^2}\right)\sin\beta_{Pc} \\
\times\cos\beta_{Pc}u_i\left(\frac{b^2}{d^2} - 1\right)
\end{array}
\\ \hline
\begin{array}{l}
- \left(\frac{\gamma I_{\eta\eta}}{AL^2}\right)\sin\beta_{Pc} \\
\times\cos\beta_{Pc}v_i\left(\frac{b^2}{d^2} - 1\right)
\end{array}
\\ \hline
\begin{array}{l}
- f_1\cos^2\beta_{Pc}S8_i \\
- \gamma\cos^2\beta_{Pc}S_i
\end{array}
\end{array}\right\}
$$

The mass, gyroscopic and stifness matrices resulting from the perturbation equations are designated $[\underset{\sim}{M}]$, $[\underset{\sim}{C}]$ and $[\underset{\sim}{K}]$ respectively, and are presented in the following:

$$[\underset{\sim}{M}] = \left[\begin{array}{c|c|c} \delta_{ij} & 0 & 0 \\ \hline 0 & \delta_{ij} & 0 \\ \hline 0 & 0 & \delta_{ij} \end{array}\right]$$

$$[\underset{\sim}{C}] = \left[\begin{array}{c|c|c} 0 & \begin{array}{l} 2 \sin \beta_{Pc} \delta_{ij} - \\ - 2 \cos \beta_{Pc} \sum_k w_{ok}(D_{ikj} - E_{ikj}) \end{array} & 0 \\ \hline \begin{array}{l} - 2 \sin \beta_{Pc} \delta_{ij} \\ - 2 \cos \beta_{Pc} \sum_k w_{ok} A_{ijk} \end{array} & \begin{array}{l} - 2 \cos \beta_{Pc} \sum_k v_{ok}(D_{ikj} - E_{ikj}) \\ - 2 \cos \beta_{Pc} \sum_k v_{ok} A_{ijk} \end{array} & 0 \\ \hline 0 & 0 & 0 \end{array}\right]$$

$$
[K] = \left[\begin{array}{l|l|l}
\begin{array}{l}
- \sin^2 \beta_{Pc}\, \delta_{ij} - \cos^2 \beta_{Pc}(B_{ij} - C_{ij}) \\
- \sin \beta_{Pc} \cos \beta_{Pc} \sum_k w_{ok} A_{ijk} + \\
\sin \beta_{Pc} \cos \beta_{Pc} \sum_k w_{ok}\left[D_{ijk} + D_{ikj} - E_{ijk} - E_{ikj}\right] \\
+ \xi\left[F_{ij} + 2\gamma\left(\frac{b^2}{d^2} - 1\right)(G_{ij} + \gamma H_{ij})\right] \\
+ f_{11} \sum_k \varphi_{ok} T2_{ikj}
\end{array} &
\begin{array}{l}
- \sin \beta_{Pc} \cos \beta_{Pc} \sum_k v_{ok} A_{ijk} \\
+ \xi\left[\frac{1}{2} I_{ij} + 2\gamma(J_{ij} - \gamma K_{ij})\right]\left(\frac{b^2}{d^2} - 1\right) \\
- f_{10} \sum_k \varphi_{ok} T1_{ikj} \\
+ f_{11} \sum_k \varphi_{ok} T3_{ikj}
\end{array} &
\begin{array}{l}
- f_{10} \sum_k v_{ok} T1_{ijk} \\
+ f_{11} \sum_k w_{ok} T2_{ijk} \\
+ f_{11} \sum_k v_{ok} T3_{ijk}
\end{array} \\
\hdashline
\begin{array}{l}
\sin \beta_{Pc} \cos \beta_{Pc} \sum_k v_{ok}(D_{ikj} - E_{ikj}) \\
+ \xi\left[\frac{1}{2} I_{ij} + 2\gamma J_{ij} - 2\gamma^2 K_{ij}\right]\left(\frac{b^2}{d^2} - 1\right) \\
+ f_{10} \sum_k \varphi_{ok} T4_{ikj} \\
+ f_{11} \sum_k \varphi_{ok} T3_{ikj}
\end{array} &
\begin{array}{l}
- \delta_{ij} - \cos \beta_{Pc}(B_{ij} - C_{ij}) \\
+ \sin \beta_{Pc} \cos \beta_{Pc} \sum_k w_{ok}(D_{ijk} - E_{ijk}) \\
+ \xi\left[M_{ij} - 2\gamma\left(\frac{b^2}{d^2} - 1\right)(G_{ij} + \gamma H_{ij})\right] \\
- f_{11} \sum_k \varphi_{ok} T2_{ikj}
\end{array} &
\begin{array}{l}
f_{10} \sum_k w_{ok} T4_{ijk} \\
+ f_{11} \sum_k w_{ok} T3_{ijk} \\
- f_{11} \sum_k v_{ok} T2_{ijk}
\end{array} \\
\hdashline
\begin{array}{l}
\sin \beta_{Pc} \cos \beta_{Pc} \sum_k \varphi_{ok}(T5_{ikj} - T6_{ikj}) \\
- \sin \beta_{Pc} \cos \beta_{Pc} \gamma O_{ji} + f_7 \sum_k v_{ok} T8_{ikj} \\
- 2\gamma f_8 \sin \beta_{Pc} \cos \beta_{Pc} S6_{ij} \\
- 2f_1 \sin \beta_{Pc} \cos \beta_{Pc} S2_{ij} \\
+ f_9 \sum_k v_{ok} T9_{ikj} - 2f_9 \sum_k w_{ok} T10_{ikj}
\end{array} &
\begin{array}{l}
f_7 \sum_k w_{ok} T8_{ijk} \\
- f_1 \sin \beta_{Pc} \cos \beta_{Pc} S7_{ij} \\
+ f_9 \sum_k w_{ok} T9_{ijk} \\
- 2f_9 \sum_k v_{ok} T10_{ijk}
\end{array} &
\begin{array}{l}
f_1 \cos^2 \beta_{Pc} S1_{ij} \\
+ f_4 S4_{ij} + \sin \beta_{Pc} \cos \beta_{Pc} \times \\
\sum_k w_{ok}(T5_{ijk} - T6_{ijk}) \\
- \cos^2 \beta_{Pc} S5_{ij} \\
+ 2\gamma f_5 \sum_k \varphi_{ok}(T7_{ijk} + T7_{ikj}) \\
- R_{ij}(\gamma^2 f_5 - f_6 - f_7 + f_8 \cos^2 \beta_{Pc})
\end{array}
\end{array}\right]
$$

APPENDIX B - NOMENCLATURE

A	cross-sectional area of blade
A_{ijk}, B_{ij}, L_i, etc.	modal integrals (see appendix A)
b, d	breadth (chord) and thickness of blade
d/b	thickness ratio
$\{B\}$, $\{X\}$, $\{X_o\}$	vectors
$[\underset{\sim}{C}]$	modal damping matrix (gyroscopic matrix)
E	Young's modulus
$f_1, \ldots f_{11}$	coefficients (see eq. (13)
G	shear modulus
i, j, k	dummy indices
I_p	polar second moment of area about centroid
$I_{\eta\eta}$, $I_{\xi\xi}$	area moments of inertia about major and minor principal centroidal axes
J	torsional stiffness constant
k_A	blade cross section polar radius of gyration
k_m	blade cross section mass radius of gyration
k_{m1}, k_{m2}	principal mass radii of gyration
L	length of beam
$[\underset{\sim}{L}]$, $[\underset{\sim}{L}N]$	Linear and nonlinear components of the matrix representing steady state equilibrium equations
m	mass of blade per unit length
$[\underset{\sim}{M}]$	modal mass matrix
n	number of nonrotating modes for each of the flatwise bending, edgewise bending, and torsional deflections
p	natural radian frequency
R	radius of disc
T	blade tension

t	time
u, v, w	displacements of the elastic axis in X, Y, Z directions, respectively
$\bar{v}, \bar{w}, \varphi$	dimensionless bending and torsional deflections
$v_{oj}, w_{oj}, \varphi_{oj}$	steady-state equilibrium quantities
x	running coordinate along X-axis
y, z	centroidal principal axes of beam cross section
α	setting angle (collective pitch)
$\alpha_j, \beta_j, \gamma_j$	constants for assumed mode shapes
β_{pc}	precone angle
γ	total pretwist of the blade over its length
$\Delta v_j, \Delta w_j, \Delta\varphi_j$	perturbation quantities
δ_{ij}	Kronecker delta
η	nondimensional length coordinate, x/L
θ	geometric pitch angle, $\alpha + \gamma\eta$
$\theta_j(\eta)$	nonrotating torsional mode shape
θ_{pt}	pretwist at a distance η from root, $\gamma\eta$
λ_1	frequency parameter, $\sqrt{EI_{\eta\eta}/\rho AL^4}$
ξ	nondimensional rotational parameter, $EI_{\eta\eta}/\rho AL^4\Omega^2$
ρ	mass density of blade material
τ	dimensionless time, Ωt
$\Psi_j(\eta)$	nonrotating flatwise and edgewise bending mode shapes
ω_1	exact fundamental mode frequency of straight, nonrotating beam, 3.51602 λ_1
Ω	rotor blade angular velocity, rad/sec
$(\ )'$	primes denote differentiation with respect to x or η
$(\dot{\ })$	dot over a parameter represents differentiation with respect to t or τ

REFERENCES

1. Hodges, D.H.; and Dowell, E.H.: Nonlinear Equations of Motion for the Elastic Bending and Torsion of Twisted Nonuniform Rotor Blades. NASA TN-D-7818, 1974.

2. Rosen, A.; and Friedmann, P.P.: Nonlinear Equations of Equilibrium for Elastic Helicopter or Wind Turbine Blades Undergoing Moderate Deformation. (UCLA-ENG-7718, University of California, Los Angeles; NASA Grant NSG-3082) NASA CR-159478, 1978.

3. Kaza, K.R.V.; and Kvaternik, R.G.: Nonlinear Aeroelastic Equations for Combined Flapwise Bending, Chordwise Bending, Torsion, and Extension of Twisted Non-Uniform Rotor Blades in Forward Flight. NASA TM-74059, 1977.

4. Kvaternik, R.G.; White, W.F. Jr.; and Kaza, K.R.V.: Nonlinear Flap-Lag-Axial Equations of a Rotating Beam with Arbitrary Precone Angle. AIAA Paper 78-491, 1978.

5. Stephens, W.B., et al: Stability of Nonuniform Rotor Blades in Hover Using a Mixed Formulation. European Rotorcraft and Powered Lift Aircraft Forum, 6th, University of Bristol, 1980.

6. Crespo da Silva, M.R.M.: Flap-Lag-Torsional Dynamic Modelling of Rotor Blades in Hover and in Forward Flight, Including the Effect of Cubic Nonlinearities. (ASD-81-6-1, Cincinnati Univ.; NASA Grant NAG2-38) NASA CR-166194, 1981.

7. Hodges, D.H.: Nonlinear Equations for Dynamics of Pretwisted Beams Undergoing Small Strains and Large Rotations. NASA TP-2470, 1985.

8. Mehmed, O., et al: Bending-Torsion Flutter of a Highly Swept Advanced Turboprops. NASA TM-82975, 1981.

9. Srinivasan, A.V.; Kielb, R.E.; and Lawrence, C.: Dynamic Characteristics of an Assembly of Prop-Fan Blades. ASME Paper No. 85-GT-134, Mar. 1985.

10. Subrahmanyam, K.B.; and Kaza, K.R.V.: Vibration and Buckling of Rotating, Pretwisted, Preconed Beams Including Coriolis Effects. Vibrations of Blades and Bladed Disc Assemblies, R.E. Kielb and N.F. Rieger, eds., ASME, 1985, pp. 75-87.

11. Subrahmanyam, K.B.; and Kaza, K.R.V.: Nonlinear Flap-Lag-Extensional Vibrations of Rotating, Pretwisted, Preconed Beams Including Coriolis Effects. NASA TM-87102, 1985.

12. Kaza, K.R.V.; and Kielb, R.E.: Effects of Warping and Pretwist on Torsional Vibration of Rotating Beams. J. Appl. Mech., vol. 51, no. 4, Dec. 1984, pp. 913-920.

13. Subrahmanyam, K.B.; and Kaza, K.R.V.: Finite Difference Analysis of Torsional Vibrations of Pretwisted, Rotating, Cantilever Beams with Effects of Warping. J. Sound Vibr., vol. 99, no. 2, Mar. 22, 1985, pp. 213-224.

14. Mil, M.L., et al.: Helicopters: Calculation and Design, Vol. I, Aerodynamics. NASA TT-F-494, 1967, pp. 430-432.

15. Chang, Tish-Chun; and Craig, R.R., Jr.: On Normal Modes of Uniform Beams. Engineering Mechanics Research Laboratory, University of Texas, EMRL-1068, 1969.

16. Brown, G.V., et al: Lewis Research Center Spin Rig and Its Use in Vibration Analysis of Rotating Systems. NASA TP-2304, 1984.

TABLE I. - CONVERGENCE PATTERN OF FREQUENCY RATIOS (p/λ_1) OF A PRETWISTED, PRECONED, ROTATING BLADE INCLUDING SECOND DEGREE GEOMETRIC NONLINEARITIES AND CORIOLIS EFFECTS

[$\Omega/\omega_1 = 0.5$, $\beta_{pc} = 15°$, $\gamma = 30°$, $\alpha = 0°$, $\overline{R} = 0$, $d/b = 0.05$, $L/d = 200$.]

Mode number	Results from perturbation solution: Galerkin method									MSC NASTRAN (500 CQUAD4 elements)
	n = 1	n = 2	n = 3	n = 4	n = 5	n = 6	n = 7	n = 8	n = 9	
1	6.7647	3.9948	3.9770	3.9715	3.9710	3.9840	3.9755	3.9699	3.9586	3.9923
2	64.5292	38.4098	20.4184	20.1127	20.0309	20.0334	19.9880	19.9823	19.9707	20.0707
3	73.7530	55.3224	52.5086	52.3541	52.4005	53.3161	51.8719	51.6155	51.4160	57.7067
4	-------	87.9097	83.8938	61.4177	60.3757	58.1215	59.7126	60.1018	60.1548	64.5911
5	-------	206.4990	137.3498	85.8415	85.3058	84.9539	86.2480	86.5334	86.7023	86.1357
6	-------	438.1967	205.3006	205.2917	123.9113	123.4958	121.5896	120.8147	120.6553	121.1038
7	-------	--------	345.6017	274.0265	205.4352	198.2435	198.2884	199.2196	199.0793	199.4268
8	-------	--------	457.0644	343.8727	343.0762	343.5164	205.8776	204.6820	204.3840	219.5793

TABLE II. - CONVERGENCE PATTERN OF STEADY-STATE TIP DEFLECTIONS

[$\Omega/\omega_1 = 0.5$, $\beta_{pc} = 15°$, $\gamma = 30°$, $\alpha = 0°$, $\overline{R} = 0$, $d/b = 0.05$.]

Method	Number of assumed modes or CQUAD4 elements	Steady-state tip deflection (center line deflection)		
		$\overline{w}$	$\overline{v}$	φ
Galerkin	n = 1	-0.018471	0.0018304	-0.0044147
	n = 2	-0.054886	0.0065991	-0.0016439
	n = 3	-0.054606	0.0058486	-0.0012554
	n = 4	-0.054841	0.0058761	-0.0011558
	n = 5	-0.054832	0.0058467	-0.0011435
MSC NASTRAN	500 elements	-0.054309	0.0058372	-0.0010209

TABLE III. - COMPARISON OF THEORETICAL AND EXPERIMENTAL RESULTS

[$d/b = 0.05$, $L/d = 60$, $\gamma = 0°$, $L = 152.4$ mm, $E = 32.3 \times 10^6$ psi, $G = 13.8 \times 10^6$ psi, $\rho = 0.283$ lb/in^3.]

β_{pc}, degree	α, degree	Ω, rpm	Method	Frequency, Hz				
				Mode 1	Mode 2	Mode 3	Mode 4	Mode 5
45	90	1800	(a)	94.6	573.4	594.6	1656.2	1883.1
			(b)	95.5	571.0	599.0	1657.0	1798.0
		4200	(a)	95.7	565.3	620.3	1669.7	1824.4
			(b)	100.0	545.0	640.0	1650.0	1823.0
		5400	(a)	95.8	557.3	641.1	1675.2	1838.6
			(b)	100.0	522.0	675.0	1642.0	1854.0
0	30	3600	(a)	126.4	582.2	623.9	1683.4	1825.8
			(b)	129.0	570.0	630.0	1688.0	1807.0
		4800	(a)	146.5	588.7	647.0	1700.4	1837.4
			(b)	146.0	582.0	665.0	1716.0	1817.0
		6000	(a)	168.6	597.0	673.4	1714.1	1853.3
			(b)	166.0	587.0	706.0	-------	-------
22.5	90	2400	(a)	101.4	574.3	603.5	1665.4	1815.8
			(b)	101.9	571.4	602.9	1664.0	1799.0
		4800	(a)	120.1	573.3	644.2	1700.6	1836.1
			(b)	121.2	562.0	654.0	1684.0	1826.0
		6000	(a)	131.8	572.3	673.3	1721.9	1855.1
			(b)	134.5	553.0	688.0	1695.0	1854.0
45	0	870	(a)	94.8	570.2	591.0	1653.1	1780.5
			(b)	95.9	574.0	588.0	1655.0	1799.0
		1506	(a)	96.3	541.0	593.0	1655.0	1675.0
			(b)	98.6	569.0	589.0	1662.0	1803.0
22.5	60	1200	(a)	96.5	572.5	593.4	1655.3	1796.3
			(b)	97.0	574.0	------	-------	1798.0
		3600	(a)	111.5	489.9	625.2	1569.0	1684.5
			(b)	124.4	561.0	626.0	-------	------
0	0	0	(a)	94.2	573.7	590.0	1652.0	1810.0
			(b)	94.2	572.0	586.0	1655.0	1795.0

[a]Present theoretical results.
[b]Experimental result.

TABLE IV. - COMPARISON OF FREQUENCY RATIOS OF PRETWISTED, PRECONED, ROTATING BLADES OF VARIOUS THICKNESS RATIOS

[α = 0°, $\bar{R}$ = 0, L/b = 10, geometric nonlinearities included.]

d/b	γ, degree	β_{pc}, degree	Ω/ω_1	Method	Method Frequency ratio, ρ/λ_1					
					Mode 1	Mode 2	Mode 3	Mode 4	Mode 5	Mode 6
0.10	0	15	0.8	(a)	4.6097	23.1186	30.4598	62.7814	68.0725	122.0243
				(c)	4.6430	23.1970	31.9459	62.8686	72.0478	122.3435
			1.0	(a)	5.1488	23.7212	27.7385	63.3946	68.1157	122.6629
				(c)	5.1750	23.7841	30.7285	63.3849	73.5597	122.8331
			2.0	(a)	8.3781	21.3722	28.3088	68.3325	70.3606	127.9158
				(c)	8.3327	28.3285	28.7811	68.0478	75.6988	127.4200
0.25	0	45	0.8	(a)	3.9975	12.5710	22.7272	61.8443	62.4559	91.0506
				(b)	4.1057	12.2505	22.7240	61.8860	62.4029	91.0091
				(c)	4.2598	12.8590	22.6460	61.3970	67.2376	89.0158
0.25	0	45	1.0	(a)	4.4286	11.0558	23.2294	59.4052	62.9189	92.1810
				(b)	4.6184	10.6218	23.2097	59.4123	62.8856	92.1343
				(c)	4.8122	12.3085	23.0257	61.0894	67.1483	91.2117
0.06	0	15	0.5	(a)	3.9654	22.4572	48.9361	62.1175	72.6927	121.3362
				(c)	3.9866	22.5073	52.2357	62.1740	75.2841	121.4498
0.06	0	45	0.5	(a)	3.6499	22.2620	Unstable	61.9376	75.9085	121.1543
				(c)	3.7055	22.2822	40.7961	61.7824	85.4823	121.0251
0.05	30	15	0.5	(a)	3.9710	20.0309	52.4005	60.3757	85.3085	123.9113
				(c)	3.9923	20.0707	57.7067	64.5911	86.1357	121.1038
0.05	30	15	1.0	(a)	5.1659	21.7959	Unstable	61.0581	86.4133	125.2654
				(c)	5.1656	20.9982	49.2750	61.8346	92.8652	121.8441
0.20	30	15	1.0	(b)	5.1411	15.4978	26.0439	60.8242	67.1784	113.9297
				(c)	5.1619	15.5424	26.0745	60.7458	70.4579	109.2493
0.20	30	45	0.8	(b)	4.0862	12.9163	23.3475	58.2695	64.4610	114.5998
				(c)	4.2651	14.2839	24.4469	58.7436	73.0801	110.8504
0.20	30	45	1.0	(b)	0.1533	7.2997	19.0724	54.6244	63.4657	--------
				(c)	Unstable	9.1287	18.2334	49.9820	84.9760	--------
0.05	30	45	0.8	(a)	Unstable	-------	--------	-------	-------	--------
				(c)	Unstable	-------	--------	-------	-------	--------

[a]Present beam theory including Coriolis effects.
[b]Present beam theory ignoring Coriolis effects.
[c]MSC NASTRAN results ignoring Coriolis effects.

TABLE V. - COMPARISON OF NONLINEAR FREQUENCY RATIOS AND STEADY-STATE DEFLECTIONS OF A PRECONED BLADE AT VARIOUS ROTATIONAL SPEEDS

[$\alpha = 0^\circ$, $\gamma = 0^\circ$, $\bar{R} = 0^\circ$, $\beta_{pc} = 15^\circ$, L/b = 10, d/b = 0.05, Coriolis effects not included. Unstable as negative p^2 obtained for I torsional frequency.]

Ω/ω_1	Method	Frequency ratio, p/λ_1						Steady-state tip deflections		
		Mode 1 (F1)	Mode 2 (F2)	Mode 3 (F3)	Mode 4 (T1)	Mode 5 (S1)	Mode 6 (F4)	$\bar{w}$	$\bar{v}$	φ
0.1	(a)	3.5344	22.0513	61.7139	68.5155	70.5703	120.9191	-0.002803	------------	------------
	(b)	3.5594	22.1618	61.9851	68.1727	70.1475	121.4925	-0.002767	------------	------------
0.3	(a)	3.6805	22.1860	61.8476	62.9968	74.5192	121.0572	-0.02326	------------	------------
	(b)	3.7062	22.2934	62.1044	63.9497	74.0049	121.6067	-0.02297	------------	------------
0.5	(a)	3.9654	22.4573	62.1175	50.3754	79.1494	121.3362	-0.05572	------------	------------
	(b)	3.9950	22.5585	62.3354	57.2115	79.8750	121.8374	-0.05500	------------	------------
0.8	(a)	4.6098	23.1186	62.7814	Unstable	82.3113	122.0243	-0.10620	------------	------------
	(b)	4.6451	23.2026	62.8837	48.1742	86.2660	122.3773	-0.10463	------------	------------
1.0	(a)	5.1448	23.7213	63.3947	Unstable	82.2947	122.6629	-0.13383	------------	------------
	(b)	5.1781	23.7926	63.4078	44.2514	88.2218	122.8856	-0.13173	------------	------------
2.0	(a)	8.3781	28.3089	68.3326	Unstable	81.0269	127.9159	-0.20305	------------	------------
	(b)	8.3385	28.3445	68.0883	39.0512	87.6030	127.5273	-0.20001	------------	------------
3.0	(a)	11.8998	34.6488	75.8305	Unstable	82.1026	136.2440	-0.22464	------------	------------
	(b)	11.7580	34.6610	75.5539	34.6610	84.4642	135.4860	-0.22205	------------	------------

[a]Present beam theory.
[b]MSC NASTRAN results ignoring Coriolis effects.

TABLE VI. - FREQUENCY RATIOS AND STEADY-STATE DEFLECTIONS OF A PRECONED BLADE NEGLECTING MIL'S TERMS

[$\alpha = \gamma = 0^\circ$, $B_{pc} = 15^\circ$, $\bar{R} = 0$, d/b = 0.05, L/b = 10, $T2_{ijk} = T3_{ijk} = T9_{ijk} = T10_{ijk} \equiv 0$. Coriolis effects ignored.]

Ω/ω_1	Mode 1	Mode 2	Mode 3	Mode 4	Mode 5	Mode 6	$\bar{w}$	$\bar{v}$	φ
0.1	3.5344	22.0513	61.7139	68.7889	70.3204	120.9191	-0.002803	-	-
0.3	3.6805	22.1860	61.8476	68.8022	70.3218	121.0572	-0.02326	-	-
0.5	3.9654	22.4573	62.1175	68.8274	70.3263	121.3362	-0.05572	-	-
0.8	4.6098	23.1186	62.7814	68.8879	70.3394	122.0243	-0.10620	-	-
1.0	5.1448	23.7213	63.3947	68.9454	70.3505	122.6629	-0.13383	-	-
2.0	8.3781	28.3089	68.3326	69.4571	70.4161	127.9159	-0.20305	-	-
3.0	11.8998	34.6488	70.2570	70.5750	75.8305	136.2440	-0.22464	-	-

TABLE VII. - EFFECT OF IGNORING CERTAIN NONLINEAR TERMS ON THE FREQUENCY RATIOS, p/λ_1, OF ROTATING, PRECONED BLADES

[$d/b = 0.06$, $L/b = 10$, $\alpha = \gamma = 0^\circ$, $\overline{R} = 0$, $\Omega/\omega_1 = 0.5$. Coriolis effects included.]

β_{pc}, degree	Mode number	$T5_{ijk} = T6_{ijk} = 0$	$T1_{ijk} = T4_{ijk} = T8_{ijk} = 0$	$T3_{ijk} = T9_{ijk} = 0$	$T1_{ijk}$ through $T10_{ijk}$ are 0	$A_{ijk} = 0$, $T1_{ijk}$ through $T10_{ijk}$ are 0	$A_{ijk} = D_{ijk} = E_{ijk} = 0$ $T1_{ijk}$ to $T10_{ijk} = 0$	All nonlinear terms ignored
15	1	3.9650	3.9650	3.9651	3.9651	3.9592	3.9475	3.9475
	2	22.4572	22.4572	22.4572	22.4572	22.4563	22.4497	22.4497
	3	48.9396	48.8668	58.6064	58.6070	58.6092	58.6104	58.6104
	4	62.1176	62.1176	62.1186	62.1186	62.1171	62.1113	62.1113
	5	72.6937	72.7639	68.8350	68.8341	68.8342	68.8342	68.8342
	6	121.3362	121.3362	121.3362	121.3362	121.3360	121.2972	121.2972
45	1	3.6558	3.6557	3.6474	3.6474	3.6171	3.5543	3.5543
	2	22.2614	22.2614	22.2614	22.2614	22.2573	22.2251	22.2251
	3	Unstable	Unstable	58.6235	58.6273	58.6368	58.6426	58.6426
	4	61.9371	61.9371	61.9412	61.9412	61.9360	61.9076	61.9076
	5	75.9208	76.1321	68.8184	68.8141	68.8141	68.8141	68.8141
	6	121.1544	121.1544	121.1544	121.1190	121.1187	121.1255	121.1255

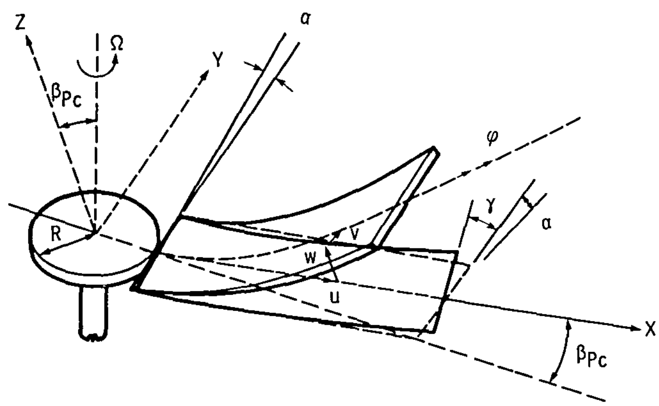

Figure 1. - Blade coordinate system and definition of blade parameters.

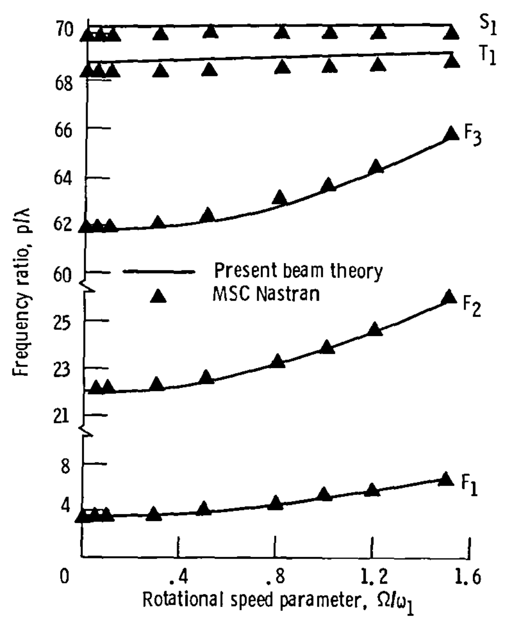

(a) $\frac{d}{b} = 0.05$, $\alpha = \gamma = \beta_{pc} = 0^0$, $\bar{R} = 0$

Figure 2. - Comparison of frequency ratios from present beam theory and MSC/NASTRAN.

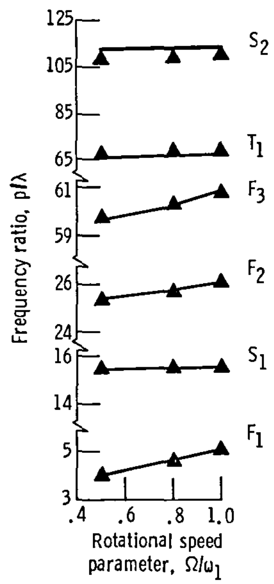

(b) $\frac{d}{b} = 0.20,\ \alpha = \gamma = 0^0,\ \beta_{pc} = 15^0,\ \bar{R} = 0$

Figure 2. - Continued.

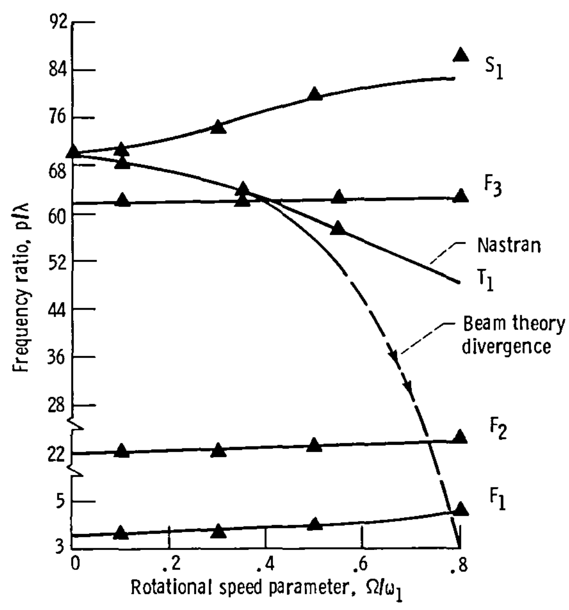

(c) $\frac{d}{b} = 0.5,\ \alpha = \gamma = 0^0,\ \beta_{pc} = 15^0,\ \bar{R} = 0$

Comparison of frequency ratio

Figure 2. - Concluded.

1. Report No.: NASA TM-87207
2. Government Accession No.:
3. Recipient's Catalog No.:
4. Title and Subtitle: Nonlinear Bending-Torsional Vibration and Stability of Rotating, Pretwisted, Preconed Blades Including Coriolis Effects
5. Report Date: January 1986
6. Performing Organization Code: 505-63-11
7. Author(s): K.B. Subrahmanyam, K.R.V. Kaza, G.V. Brown, and C. Lawrence
8. Performing Organization Report No.: E-2811
9. Performing Organization Name and Address: National Aeronautics and Space Administration, Lewis Research Center, Cleveland, Ohio 44135
10. Work Unit No.:
11. Contract or Grant No.:
12. Sponsoring Agency Name and Address: National Aeronautics and Space Administration, Washington, D.C. 20546
13. Type of Report and Period Covered: Technical Memorandum
14. Sponsoring Agency Code:
15. Supplementary Notes:
K.B. Subrahmanyam, on leave from NBKR Institute of Science and Technology, Mechanical Engineering Dept., Vidyanagar 524413, India and presently Senior Research Associate, University of Toledo, Toledo, Ohio 43606. Portions of this material were presented at the Workshop on Dynamics and Aeroelastic Stability Modeling of Rotor Systems cosponsored by the Army Research Office and Georgia Institute of Technology, Atlanta, Georgia, December 4-5, 1985.

16. Abstract

The coupled bending-bending-torsional equations of dynamic motion of rotating, linearly pretwisted blades are derived including large precone, second degree geometric nonlinearities and Coriolis effects. The equations are solved by the Galerkin method and a linear perturbation technique. Accuracy of the present method is verified by comparisons of predicted frequencies and steady state deflections with those from MSC/NASTRAN and from experiments. Parametric results are generated to establish where inclusion of only the second degree geometric nonlinearities is adequate. The nonlinear terms causing torsional divergence in thin blades are identified. The effects of Coriolis terms and several other structurally nonlinear terms are studied, and their relative importance is examined.

17. Key Words (Suggested by Author(s)): Nonlinear vibrations; Rotation; Pretwist; Precone; Coriolis effect; Stability
18. Distribution Statement: Unclassified - unlimited; STAR Category 39
19. Security Classif. (of this report): Unclassified
20. Security Classif. (of this page): Unclassified
21. No. of pages:
22. Price*:

*For sale by the National Technical Information Service, Springfield, Virginia 22161

End of Document